Monte Carlo study of magnetic and thermodynamic properties of a ferrimagnetic mixed-spin Ising nanotube with double (surface and core) walls

R. Masrour[a] and A. Jabar

Laboratory of Materials, Processes, Environment and Quality, Cadi Ayyad University,
National School of Applied Sciences - Sidi Bouzid, 63 46000 Safi, Morocco and
Laboratory of Solid State Physics, Faculty of Science, Sidi Mohammed Ben Abdellah University
Dhar Mahraz, BP 1796, Fez, Morocco

Abstract – Magnetic properties of Ising nanotubes with double surface and core walls were studied using Monte Carlo study. Total and partial magnetizations and magnetic susceptibilities with walls surface and in the core walls have been given. The effect of crystal field and reduced exchange interactions at surface on total magnetization at surface and core walls were studied. Magnetic hysteresis cycles with double surface and core walls have been found.

Introduction. – In previous works [1,2], magnetic nanosystems and nanotube/nanowire devices, have garnered considerable attention. The Blume-Capel model and the effective-field theory (EFT) on a cylindrical Ising nanowire have been studied [3]. The magnetic properties of nanograins of $La_{0.67}Sr_{0.3}MnO_3$ are studied using Monte Carlo simulation (MCS) [4]. Liu *et al.* [5] have used the EFT and MCS to study the mixed spins 1/2 and 2 diamond chain with the Ising model (IM). The magnetic hysteresis and thermodynamic properties of double-walled carbon nanotubes are studied [6,7]. On the other hand, triple of hysteresis cycles have been observed in spin-1/2 core and spin-1 surface [8]. Kocakaplan *et al.* have applied the effective field theory to study magnetic and thermal properties of a nanoscaled spin-1/2 hexagonal Ising nanowire [9]. Experimentally, synthesis and photoeletrochemical performance of AuAg/CdS double-walled nanotubes have been studied by ref. [10]. In a previous work [11], the hierarchical Co_3O_4/NiO core-shell nanotubes were fabricated by the deposition of NiO shells via a chemical bath treatment using electrospun Co-C composite nanofibers as templates, followed by a calcination process in air. Desmecht *et al.* [12] have studied the intact sp^2 carbon atoms followed by post-functionalization to graft a dipyridylamine ligand on the surface of both solids and pristine carbon nanotubes. In recent years, there have been breakthroughs in both experimental and theoretical investigations of magnetic nanotubes [13–15]. The core-double-shell structured magnetic halloysite nanotube nano-hybrid has been reported in ref. [16]. Some results on nanotubes may have potential applications in different research fields, such as electronics, optics, mechanics and even biomedicine and molecular devices [17,18]. The magnetic properties of diamond-shaped graphene quantum dots have been investigated by varying their sizes with the Monte Carlo simulation [19].

In the present work, magnetizations and magnetic susceptibilities with walls surface and in the core walls have been studied. Magnetic hysteresis cycles with double surface and core walls have been established. The introduction is presented in the current section. The Ising model is given in the following section. The method of simulation is illustrated in the third section. The results and discussion have been detailed in the fourth section. Finally, we have given the conclusion in the final section.

Ising model. – We consider an Ising nanowire with double surface wall and core wall the mixed spins $\sigma = 3/2$

[a]E-mail: `r.masrour@uca.ma` (corresponding author)
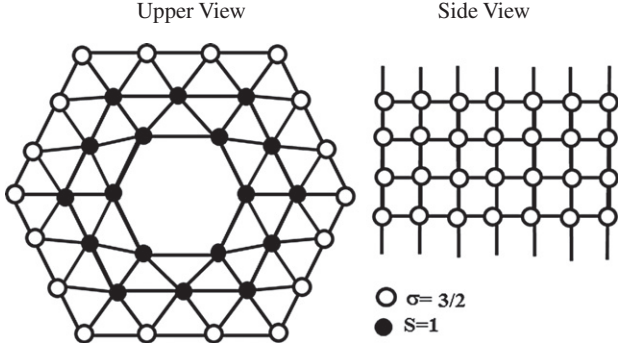
Upper View   Side View

Fig. 1: Schematic representation of the Ising nanowire with double surface and core walls. The open and black circles on each section represent the spin-3/2 and spin-1 magnetic atoms at the surface wall and in the core wall, respectively.
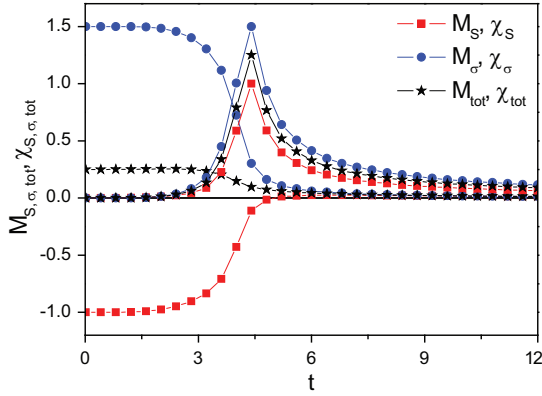

Fig. 2: The total and partial magnetizations and magnetic susceptibilities of the Ising nanowire with walls surface (M_S) wall and in the core wall (M_σ) for $r = -1.0$, $p = +1.0$, $d_S = 0$, $d_\sigma = 0$ and $h/J_{SS} = 0.2$.

and $S = 1$, respectively. The Hamiltonian of our system is given by

$$H = -\sum_{\langle i,j \rangle} S_i S_j - r \sum_{\langle i,k \rangle} S_i \sigma_k$$

$$- p \sum_{\langle k,m \rangle} \sigma_k \sigma_m - d_S \sum_i S_i^2 - d_\sigma \sum_k \sigma_k^2$$

$$- h/J_{SS} \left(\sum_i S_i + \sum_k \sigma_k \right), \qquad (1)$$

with $r = J_{S\sigma}/J_{SS}$, $p = J_{\sigma\sigma}/J_{SS}$, $d_s = \Delta_S/J_{SS}$, $d_\sigma = \Delta_\sigma/J_{SS}$ and $t = T/J_{SS}$, Δ and h are the crystal field and external field, respectively. $J_{S\sigma}$ and J_{SS} are the exchange interactions between S-σ and S-S, respectively.

The possible spin projections of $\sigma = 3/2$ and $S = 1$ spins moments are $(+3/2; +1/2; -1/2; -3/2)$ and $(+1; 0; -1)$, respectively.

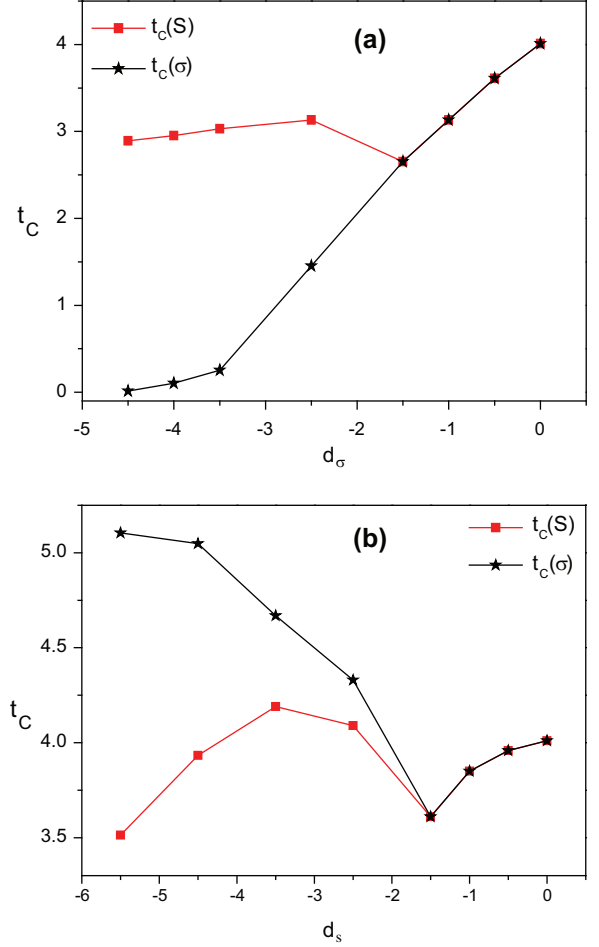**Method of simulations.** – The Ising nanowire of double surface and core walls with mixed spins 3/2 and 1 has

Fig. 3: The reduced transition temperature t_C of the Ising nanowire with walls surface (M_S) wall and in the core wall (M_σ) vs. reduced crystal field at surface (S) with $d_S = 0$ (a) and with reduced crystal field at surface (S) with $d_\sigma = 0$ (b) for $r = -1.0$, $p = +1.0$ and $h/J_{SS} = 0.2$.

been presented in fig. 1. This system is assumed to reside in the unit cells and the nanowire consists of the total number of spins $N = (N_S + N_\sigma) * L$, with $N_S = N_\sigma = 18$ and $L = 10$. The Monte Carlo simulation is applied to simulate the Hamiltonian given by eq. (1). Free boundary conditions on the lattice were imposed and the configurations were generated by sequentially traversing the lattice and making single-spin flip attempts. The flips are either accepted or rejected according to a heat-bath algorithm under the Metropolis approximation. Our data were generated with 10^5 Monte Carlo steps per spin, discarding the first 10^4 Monte Carlo simulations. Starting from different initial conditions, we performed the average of each parameter and estimated the Monte Carlo simulations, averaging over many initial conditions. Our program calculates the following parameters, namely:

The internal energy per site E of the Ising nanowire with double surface wall and core wall is

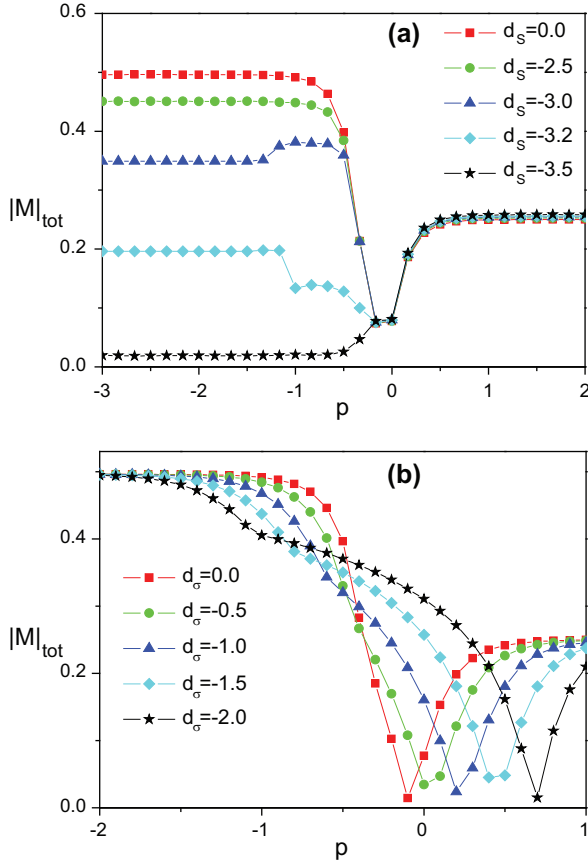$$E = \frac{1}{N} \langle H \rangle. \qquad (2)$$

Fig. 4: The total magnetization *vs.* the reduced exchange interactions at surface of the Ising nanowire with different values of reduced crystal field at surface $d_S = 0, -2.5, -3.0, -3.2, -3.5$ (a) and $d_\sigma = 0.0, -0.5, -1.0, -1.5, -2.0$ (b) for $r = -1.0$, $t = 1$ and $h/J_{SS} = 0.2$.
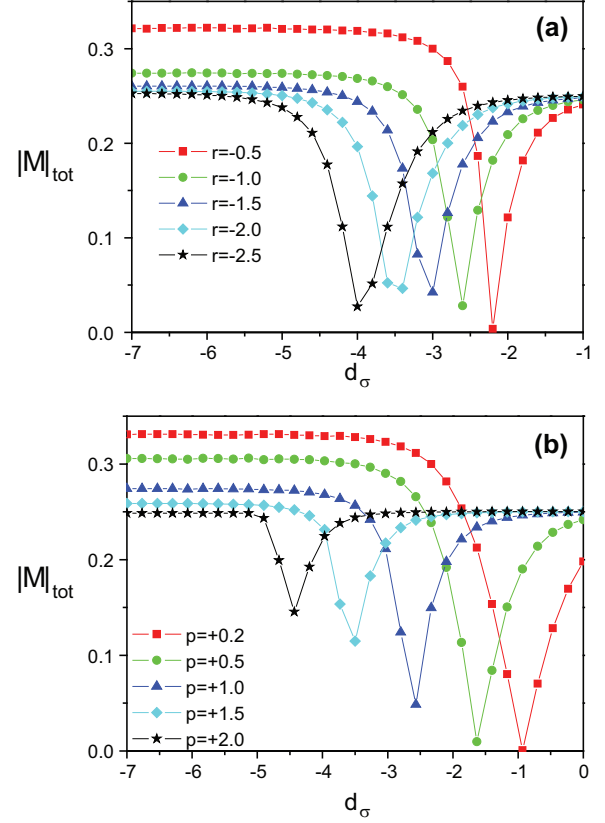

Fig. 5: The total magnetization *vs.* the reduced crystal field at surface of the Ising nanowire with different values of reduced exchange interactions between surface and core $r = -0.5, -1.0, -1.5, -2.0, -2.5$, $p = +1.0$ (a) and reduced exchange interactions between spins σ-σ, $p = +0.2, +0.5, +1.0, +1.5, +2.0$, $r = -1.0$ (b) for $d_S = 0$, $t = 1$ and $h/J_{SS} = 0.2$.

Magnetizations of the Ising nanowire with double surface wall and core wall, respectively, are

$$M_\sigma = \frac{1}{N_\sigma} \left\langle \sum_i \sigma_i \right\rangle, \tag{3}$$

$$M_S = \frac{1}{N_S} \left\langle \sum_i S_i \right\rangle. \tag{4}$$

Total magnetization of IN with double surface wall and core wall is

$$M_{tot} = \frac{N_S M_S + N_\sigma M_\sigma}{N_S + N_\sigma}. \tag{5}$$

Magnetic susceptibilities of the Ising nanowire (IN) with double surface wall and core wall are given by

$$\chi_S = \beta \left(\langle M_S^2 \rangle - \langle M_S \rangle^2 \right), \tag{6}$$

$$\chi_\sigma = \beta \left(\langle M_\sigma^2 \rangle - \langle M_\sigma \rangle^2 \right), \tag{7}$$

where $\beta = \frac{1}{k_B T}$, T denotes the absolute temperature and k_B is the Boltzmann's constant.

Total magnetic susceptibility of IN with double surface and core walls is given by

$$\chi_{tot} = \frac{N_S \chi_S + N_\sigma \chi_\sigma}{N_S + N_\sigma}. \tag{8}$$

Results and discussion. – Figure 2 displays the total and partial of magnetizations and magnetic susceptibilities of the Ising nanowire with surface and core walls for $r = -1.0$, $p = +1.0$, $d_S = 0$, $d_\sigma = 0$ and $h/J_{SS} = 0.2$. The maximums of magnetic susceptibilities are situated at reduced transition temperature $t_C = 4.4$. The system goes from ferromagnetic phase to paramagnetic phase. A second phase transition was observed at the reduced transition temperature t_C.

Figure 3(a) shows the reduced transition temperature t_C of the Ising nanowire with surface wall *vs.* reduced crystal field d_σ. Figure 3(b) gives the variation of the reduced transition temperature t_C *vs.* crystal field d_S for $r = -1.0$, $p = +1.0$ and $h/J_{SS} = 0.2$. For $d_\sigma < -1.5$, the surface is ordered before the core walls and for $d_\sigma > -1.5$, surface and core walls are ordered at the same time. The value $(d_\sigma)_C = 1.5$ can be defined as the particular d_σ value
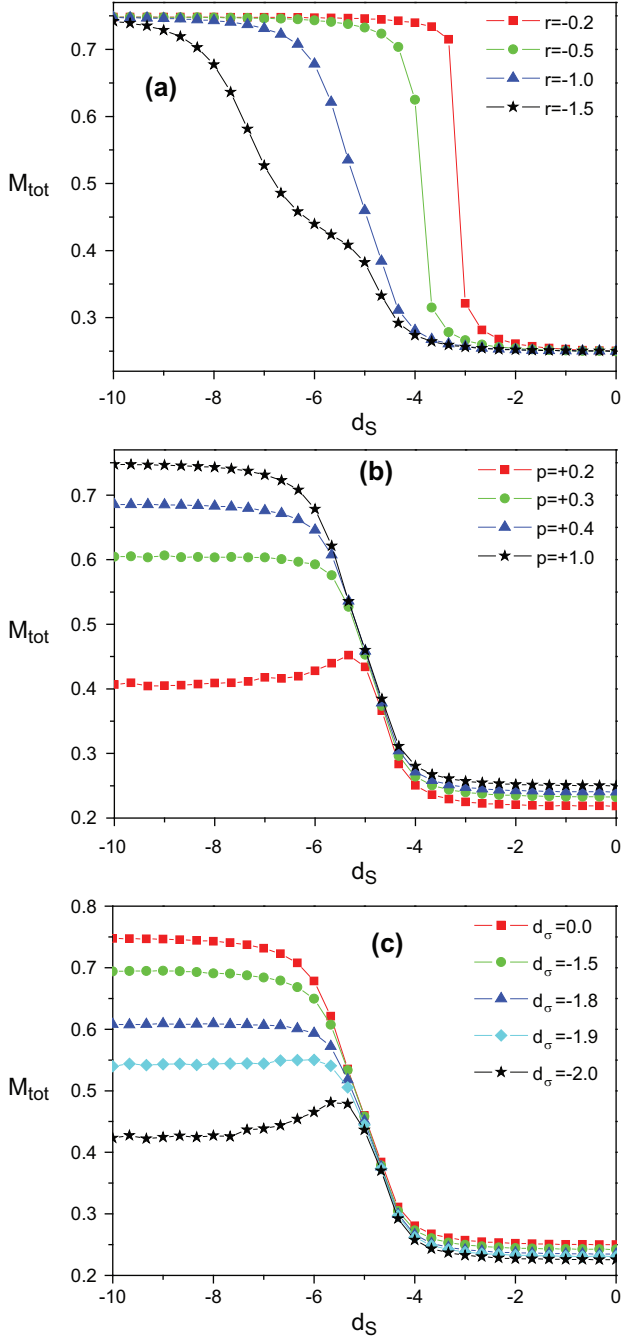
Fig. 6: The total magnetization *vs.* the reduced crystal field at core of the Ising nanowire with different values of reduced exchange interactions between surface and core $r = -0.2, -0.5, -1.0, -1.5$, $p = +1.0$ (a) and reduced exchange interactions between surface and surface $p = +0.2, +0.3, +0.4, +1.0$, $r = -1.0$ (b), with different reduced crystal field $d_\sigma = 0.0, -1.5, -1.8, -1.9, -2.0$ (c) for $t = 1$ and $h/J_{SS} = 0.2$.
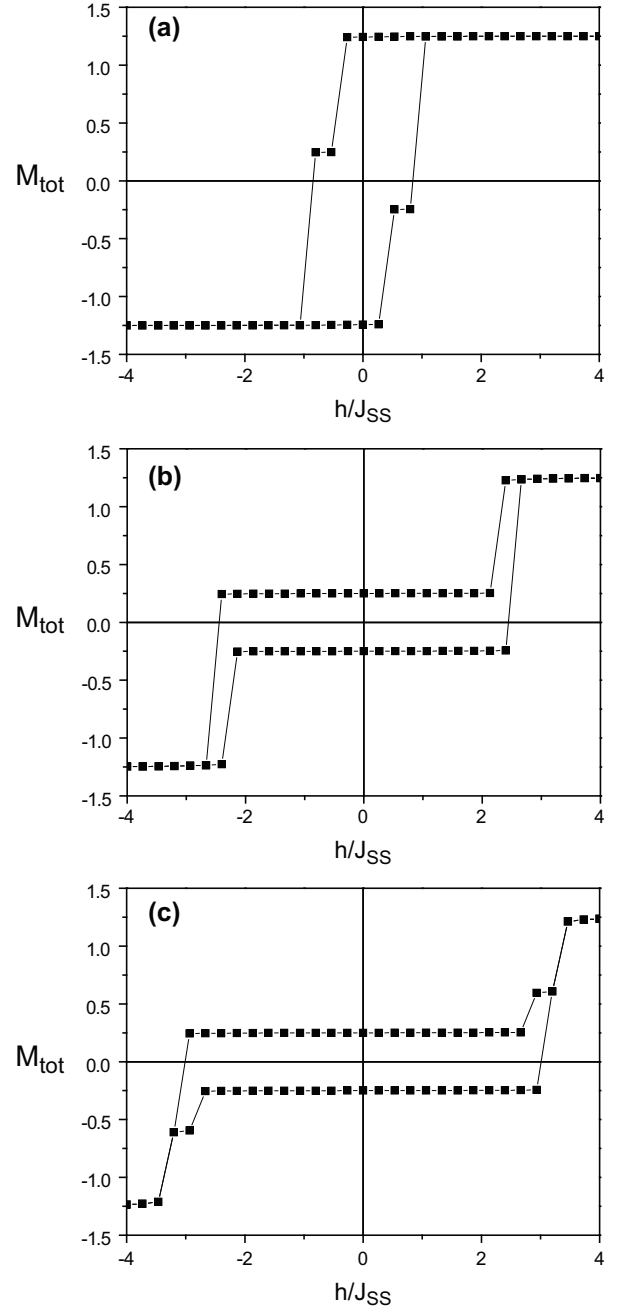
Fig. 7: The magnetic hysteresis cycles of the Ising nanowire with double surface and core walls for $r = -0.1$ (a), -1.0 (b), -1.3 (c) for $p = +1.0$, $d_S = 0$, $d_\sigma = 0$ and $t = 1$.

at which $(t_C)_\sigma = (t_C)_S$. The inverse phenomenon is observed in fig. 3(b) when $d_S < -1.5$, the surface transition for which the surface is ordered before the core walls. For $d_S > -1.5$, the behavior is similar to that obtained in fig. 3(a).

We have presented, in fig. 4, the absolute value of total magnetization *vs.* the reduced exchange interactions at surface of the Ising nanowire with different values of crystal field $d_S = 0, -2.5, -3.0, -3.2, -3.5$ (a) and $d_\sigma = 0.0, -0.5, -1.0, -1.5, -2.0$ (b) for $r = -1.0$, $t = 1$ and $h/J_{SS} = 0.2$. For $p < -1.3$, the total magnetization is constant, decreases rapidly in the $-0.49 < p < -0.15$ range and increases in the $-0.087 < p < 0.51$ range until it reaches saturation. For $p < -1.68$, the absolute value of the total magnetization is constant and decreases with absolute value of the crystal field until $p = -0.1$, 0.005,
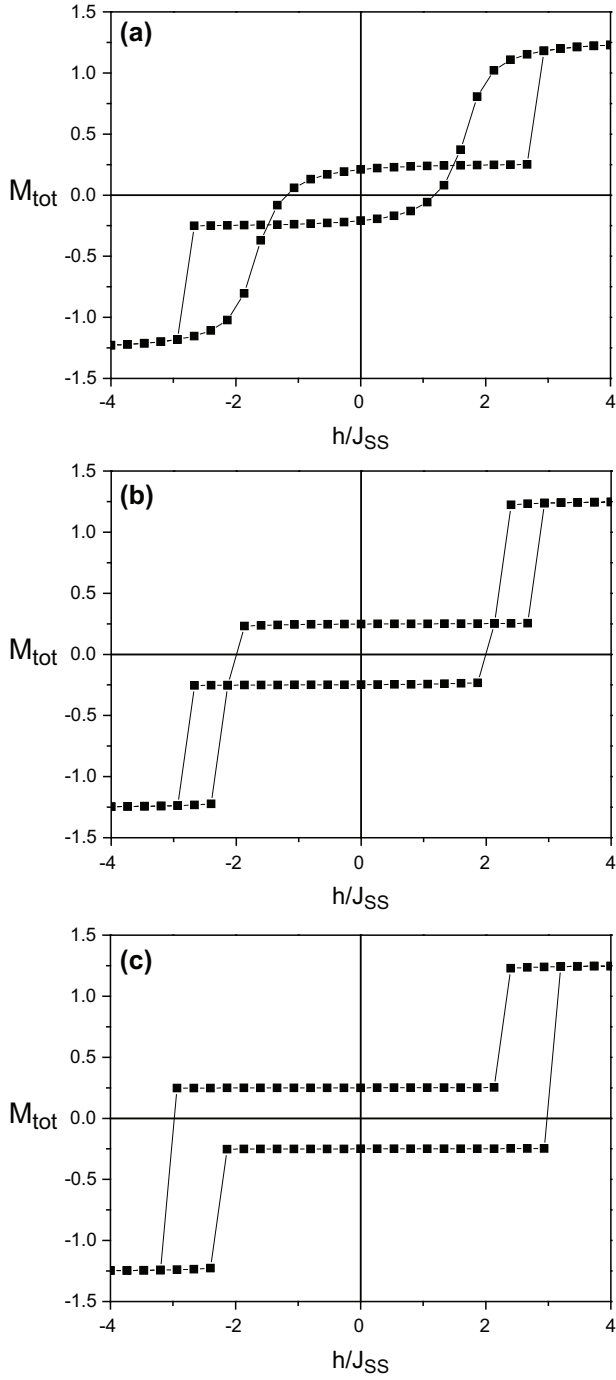
Fig. 8: The magnetic hysteresis cycles of the Ising nanowire with double surface and core walls for $p = +0.2$ (a), $+0.7$ (b), $+1.2$ (c) for $r = -1.0$, $d_S = 0$, $d_\sigma = 0$ and $t = 1$.
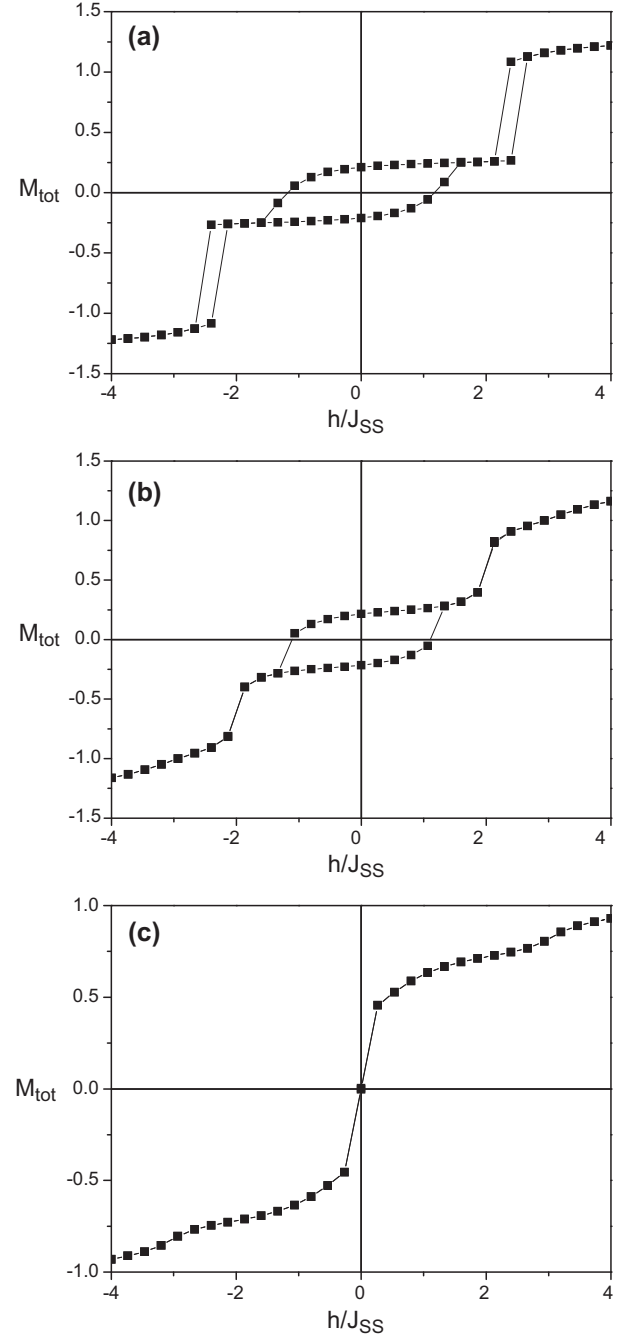

Fig. 9: The magnetic hysteresis cycles of the Ising nanowire with double surface and core walls for $d_S = -1.5$ (a), -3.0 (b), -5.0 (c) for $r = -1.0$, $p = +1.0$, $p = +0.2$, $d_\sigma = 0$ and $t = 1$.

0.02, 0.4 and 0.7 for $d_\sigma = 0.0$, -0.5, -1.0, -1.5, -2.0, respectively. After that the total magnetization increases until it reaches saturation for different values of d_σ such as given in fig. 4(a).

Figures 5(a) and (b) illustrate the absolute value of the total magnetization *vs.* the reduced crystal field at the surface of the Ising nanowire with different values of exchange interactions ($r = -0.5, -1.0, -1.5, -2.0, -2.5$

and $p = +1.0$) and ($p = +0.2, +0.5, +1.0, +1.5, +2.0$ and $r = -1.0$), respectively for $d_S = 0$, $t = 1$ and $h/J_{SS} = 0.2$. The total magnetization is constant for $d_\sigma > -1$ and $d_\sigma \leq -5$ and decreases with absolute values of r until $d_\sigma = -2.19, -2.6, -2.99, -3.61$ and -3.99 for $r = -0.5, -1.0, -1.5, -2.0, -2.5$, respectively. After that the total magnetization increases until it reaches their saturation for different values of r (see fig. 5(a)). The absolute value of total magnetization
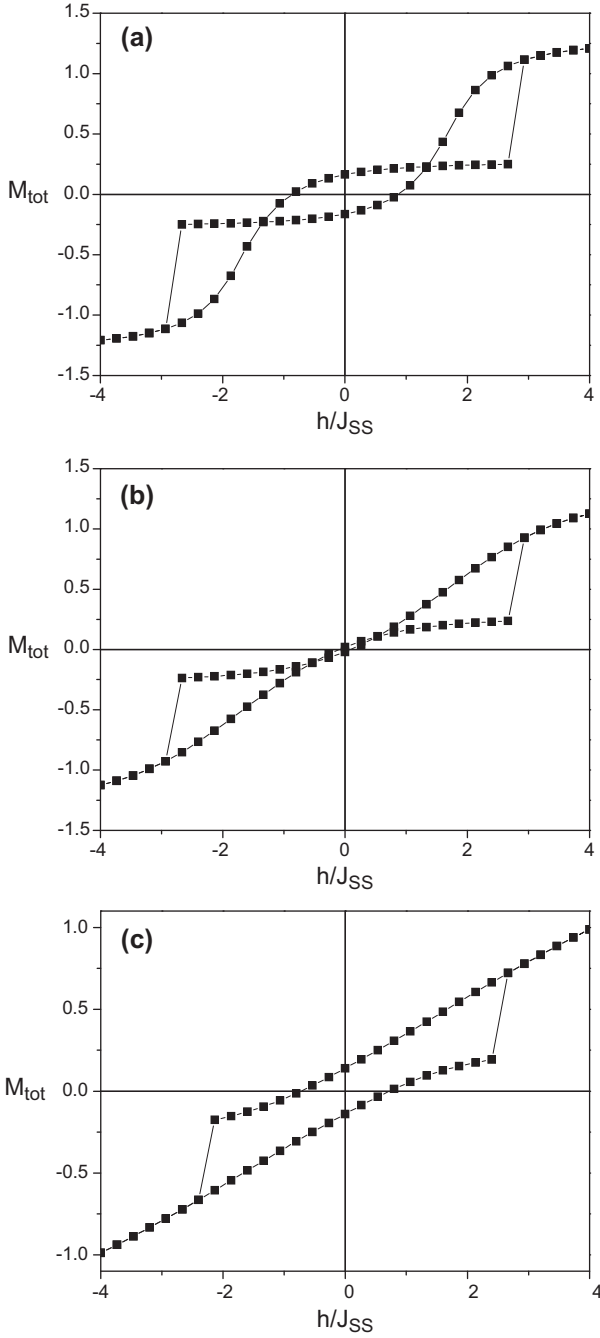
Fig. 10: The magnetic hysteresis cycles of the Ising nanowire with double surface and core walls for $d_\sigma = -0.4$ (a), -1.0 (b), -1.5 (c) for $r = -1.0$, $p = +1.0$, $p = +0.2$, $d_S = 0$ and $t = 1$.
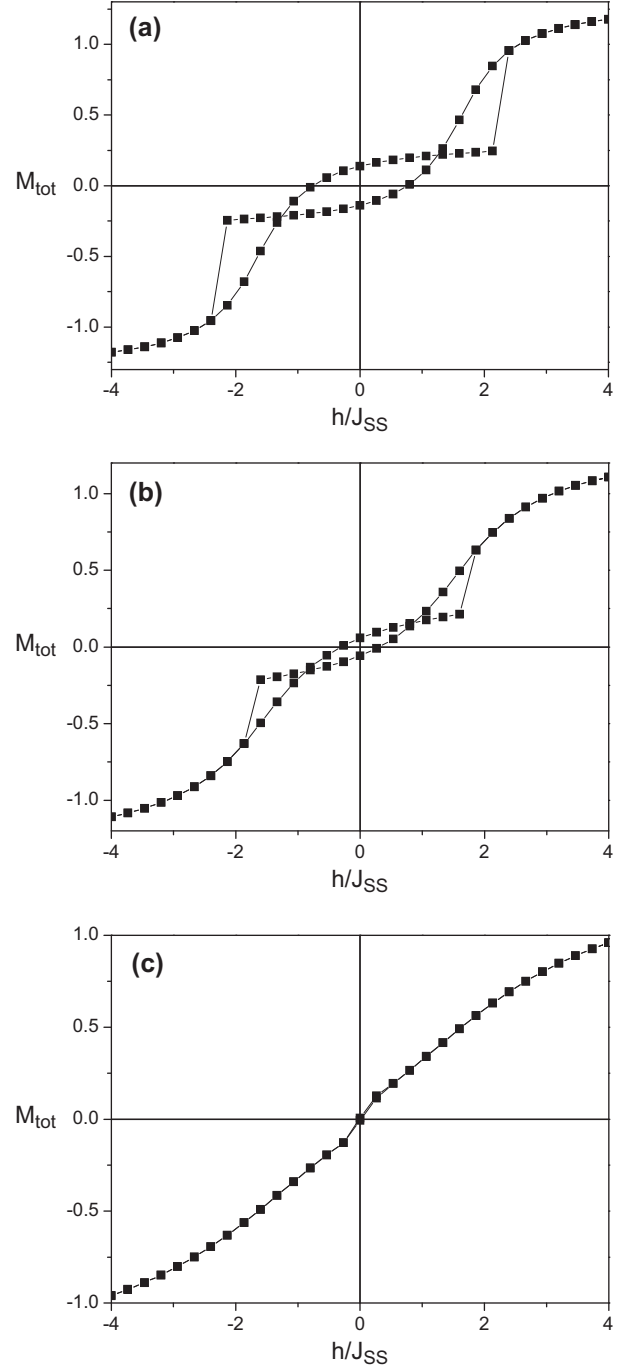

Fig. 11: The magnetic hysteresis cycles of the Ising nanowire with double surface and core walls for $t = +1.5$ (a), $+2.0$ (b), 3.0 (c) for $r = -1.0$, $p = +1.0$, $p = +0.2$, $d_S = 0$ and $d_\sigma = 0.0$.

decreases with increasing the absolute value of crystal field until $d_\sigma = -0.92, -1.62, -2.58, -3.52$ and -4.45 for $p = +0.2, +0.5, +1.0, +1.5, +2.0$, respectively. After that the total magnetization increases until it reaches their saturation for different values of p (see fig. 5(b)).

Total magnetization vs. the reduced crystal field at core with of IN with different values of reduced exchange interactions between surface and core $r = -0.2, -0.5, -1.0, -1.5$, $p = +1.0$ and reduced exchange interactions between surface-surface $p = +0.2, +0.3, +0.4$,

$+1.0$, $r = -1.0$ are given in figs. 6(a) and (b) with different reduced crystal field $d_\sigma = 0.0, -1.5, -1.8, -1.9, -2.0$ for $t = 1$ and $h/J_{SS} = 0.2$. We see that the total magnetization becomes constant for $d_S > -2$ whatever the values of r, p and d_σ and it remains constant when $d_S < -8$ and decreases rapidly elsewhere. For $(d_S)_C = -4.66$, the system does not depend on the crystal field $d_S = d_\sigma$ such as given in fig. 6(c).

Figure 7 presents the magnetic hysteresis cycles of IN with double surface and core walls for $r = -0.1$ (a), -1.0 (b), -1.3 (c) for $p = +1.0$, $d_S = 0$, $d_\sigma = 0$ and $t = 1$. The coercive field and remanent magnetization increase with increasing the absolute values of exchange interactions between surface and core walls. In a previous work [20], they found that the remanent magnetization decreases with the decreasing of shell (or surface) exchange coupling. This result is in good agreement with our results. The triple loops are composed of one central loop and two-sided symmetric loops.

Magnetic hysteresis cycles of the Ising nanowire with double surface and core walls for $p = +0.2, +0.7, +1.2$ are presented in figs. 8(a)–(c), for $r = -1.0$, $d_S = 0$, $d_\sigma = 0$ and $t = 1$. The coercive field increases with increasing the absolute values of exchange interactions between surface-surface walls.

It is shown that as p decreases the hysteresis curve changes from one central loop to triple loops.

In fig. 9, we plot the magnetic hysteresis cycles of the IN with double surface and core walls for $d_S = -1.5$ (a), -3.0 (b), -5.0 (c) for $r = -1.0$, $p = +1.0$, $p = +0.2$, $d_\sigma = 0$ and $t = 1$. It is shown that as d_S decreases the hysteresis curve changes from triple loops to one loops. The superparamagnetism behavior is observed for $d_S = -5.0$.

The magnetic hysteresis cycles of the Ising nanowire with double surface and core walls for $d_\sigma = -0.4$ (a), -1.0 (b), -1.5 (c) as shown in fig. 10, for $r = -1.0$, $p = +1.0$, $p = +0.2$, $d_S = 0$ and $t = 1$. It is shown that as d_σ decreases the hysteresis curve changes from triple loops to one loops.

Finally, we display in fig. 11 the magnetic hysteresis cycles of IN with double surface and core walls for $t = +1.5$ (a), $+2.0$ (b), 3.0 (c) for $r = -1.0$, $p = +1.0$, $p = +0.2$, $d_S = 0$ and $d_\sigma = 0.0$. It is shown that as the reduced temperature increases the hysteresis curve changes from triple loops to one loops. The system presents the superparamagnetism for $t = 3.0$. The magnetic coercive field and remanent magnetization decrease with increasing the absolute value of the crystal field and temperature values.

Conclusions. – The magnetic behavior of the nanotube with double surface and core walls has been investigated. The reduced transition temperature of this system is obtained. The system goes from ferromagnetic phase to paramagnetic phase and the second phase transition is observed at the reduced transition temperature. The order and disorder depend on crystal field and exchange interactions in the surface and in the core walls. The coercive field and remanent magnetization increase with increasing the absolute values of exchange interactions. The triple loops are composed of one central loop and two-sided symmetric loops. The magnetic coercive and magnetization remanent decrease with increasing the absolute value of crystal field and temperatures.

REFERENCES

[1] SKOMSKI R., *J. Phys.: Condens. Matter*, **15** (2003) R841.
[2] ZOU X. and XIAO G., *Phys. Rev. B*, **77** (2008) 054417.
[3] CANKO O., TAŞKIN F., ARGIN K. and ERDINÇ A., *Solid State Commun.*, **183** (2014) 35.
[4] CUCHILLO A., VARGAS P., LEVY P., SANCHEZ R. D., CURIALE J., LEYVA A. G. and TROIANI H. E., *J. Magn. & Magn. Mater.*, **320** (2008) e331.
[5] LIU W.-J., XIN Z.-H., CHEN S.-L. and ZHANG C.-Y., *Chin. Phys. B*, **22** (2013) 027501.
[6] BENHOURIA Y., ESSAOUDI I., AINANE A., AHUJA R. and DUJARDIN F., *Superlattices Microstruct.*, **75** (2014) 761.
[7] KANEYOSHI T., *J. Supercond. Nov. Magn.*, **31** (2018) 483.
[8] EL HAMRI M., BOUHOU S., ESSAOUDI I., AINANE A., AHUJA R. and DUJARDIN F., *Physica B*, **524** (2017) 137.
[9] KOCAKAPLAN Y. and KANTAR E., *Chin. Phys. B*, **23** (2014) 046801.
[10] GUAN S., FU X., TANG Y. and PENG Z., *Chem. Phys. Lett.*, **682** (2017) 128.
[11] ZHU Y., YANG Z., CHI M., LI M., WANG C. and LU X., *Talanta*, **181** (2018) 431.
[12] DESMECHT A., PENNETREAU F., LHOOST A., NIRCHA I., PICHON B. P., RIANT O. and HERMANS S., *Catal. Today*, **334** (2019) 24.
[13] ALIMOHAMMADI V., SEDIGHI M. and JABBARI E., *Ecol. Eng.*, **102** (2017) 90.
[14] KHANA U., ADEELAB N., WENJING LIA, IRFANA M., JAVEDA K., RIAZA S. and HANA X. F., *J. Magn. & Magn. Mater.*, **424** (2017) 410.
[15] MASROUR R., JABAR A., HAMEDOUN M., BENYOUSSEF A. and HLIL E. K., *J. Magn. & Magn. Mater.*, **432** (2017) 318.
[16] WAN X., ZHAN Y., LONG Z., ZENGA G. and HE. Y., *Chem. Eng. J.*, **330** (2017) 491.
[17] LIANG J. Y., ZOU C. L., JIANG W. and LI X. X., *Physica E*, **69** (2015) 81.
[18] WANG W., LIU Y., GAO Z., ZHAO X., YANG Y. and YANG S., *Physica E*, **101** (2018) 110.
[19] MASROUR R. and JABAR A., *Physica A*, **497** (2018) 211.
[20] JIANG W., LI X.-X., LIU L.-M., CHEN J.-N. and ZHANG F., *J. Magn. & Magn. Mater.*, **353** (2014) 90.